ACS OMEGA

http://pubs.acs.org/journal/acsodf

Article

Proteomic and Metabolomic Revealed Differences in the Distribution and Synthesis Mechanism of Aroma Precursors in Yunyan 87 Tobacco Leaf, Stem, and Root at the Seedling Stage

Amin Liu, Kailong Yuan, Haiqing Xu, Yonggang Zhang, Jingkui Tian, Qi Li, Wei Zhu,* and He Ye*

Cite This: *ACS Omega* 2022, 7, 33295−33306

Read Online

ACCESS | Metrics & More | Article Recommendations | Supporting Information

ABSTRACT: Tobacco, as an important cash crop and model plant, has been the subject of various types of research. The quality of flue-cured tobacco products depends on the compound collection of tobacco leaves, including pigments, carbohydrates, amino acids, polyphenols, and alkaloid aroma precursors. The present study investigates tobacco seedling organs (leaf, stem, and root) with the assistance of label-free proteomic technology and untargeted metabonomic technology. We analyzed 4992 proteins and 298 metabolites obtained in the leaf, stem, and root groups and found that there were significant differences in both primary and secondary metabolism processes involved in aroma precursor biosynthesis, such as carbohydrate metabolism, energy metabolism, and amino acid biosynthesis, and phenylpropanoid, flavonoid, and alkaloid biosynthesis. The findings showed that the contents of alkaloid metabolites such as nornicotine, anatabine, anatalline, and myosmine were significantly higher in tobacco roots than in leaves and stems at the seedling stage.

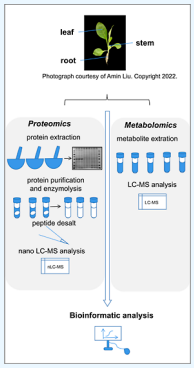

1. INTRODUCTION

Tobacco (*Nicotiana tabacum* L.), belonging to Solanaceae, is an important economic and model crop with high economic and scientific research value.[1] As a cash crop, the quality of flue-cured tobacco depends on the aroma precursors in tobacco leaves, including carbohydrates,[2] pigments,[3] polyphenols,[4] amino acids,[5] nicotine,[6] and so forth. The synthesis of these aroma precursors is closely related to the growth status.[7]

The content of aroma precursors in tobacco leaves at different periods has different characteristics. As found by Han et al., during the growth and development of tobacco, the total amount of aroma substances increased gradually with the formation of tobacco plants.[8] Tobacco cultivation at the seedling stage is an important step before transplanting into the field, and its influence on the later growth condition of tobacco in the field cannot be ignored. Tobacco leaves, stems, and roots have utility values. First, tobacco leaves are the main harvesting products for tobacco. Nicotine is an important indicator of the quality of tobacco leaves; nicotine is first synthesized in tobacco roots, then transported to the aboveground parts through the xylem and stored in the vacuole of leaves.[9] In addition, tobacco's hairy roots can express grape resveratrol *O*-methyltransferase, which can transform exogenous T-resveratrol into pterostilbene.[10] Tobacco stems were recycled in a mixed-fuel energy supply.[11,12] In addition, the roots, stems, and leaves of tobacco produce solanesol, which is an important noncyclic terpene alcohol and an anticancer drug.[13] Therefore, it is necessary for us to understand the distribution characteristics and synthesis mechanism of key aroma precursors and other important compounds in tobacco leaves, stems, and roots during the seedling stage.

With the continuous application and advancement of omics technologies, it is now possible to study tobacco proteins and metabolites at an in-depth level via proteomics and metabolomic platforms. Dai et al. (2021) studied the changes in protein regulatory pathways in the roots of flue-cured tobacco seedlings treated with high potassium compared with the normal group by using differential proteomics. High potassium stress stimulated the protein synthesis process of roots and enhanced the material metabolism pathway, thus providing a material and energy basis for root growth.[14] Wu et al. (2020) studied the molecular mechanism of chlorophyll metabolism in tobacco leaves by using the iTRAQ proteomics method and found that the upregulation of chlorophyll-like isoform X2 was a key protein regulation mechanism of chlorophyll metabolism and color change.[15] Chang et al. (2020) conducted a combined metabolomic and transcriptomic analysis of leaves of K326 at seven locations and found that the transcription factor NtGATA5 regulated carbon and nitrogen metabolism and chloroplast development by regulating plant hormones during leaf development. In addition, auxin was also studied during leaf

Received: June 21, 2022
Accepted: August 29, 2022
Published: September 8, 2022

https://doi.org/10.1021/acsomega.2c03877
ACS Omega 2022, 7, 33295−33306

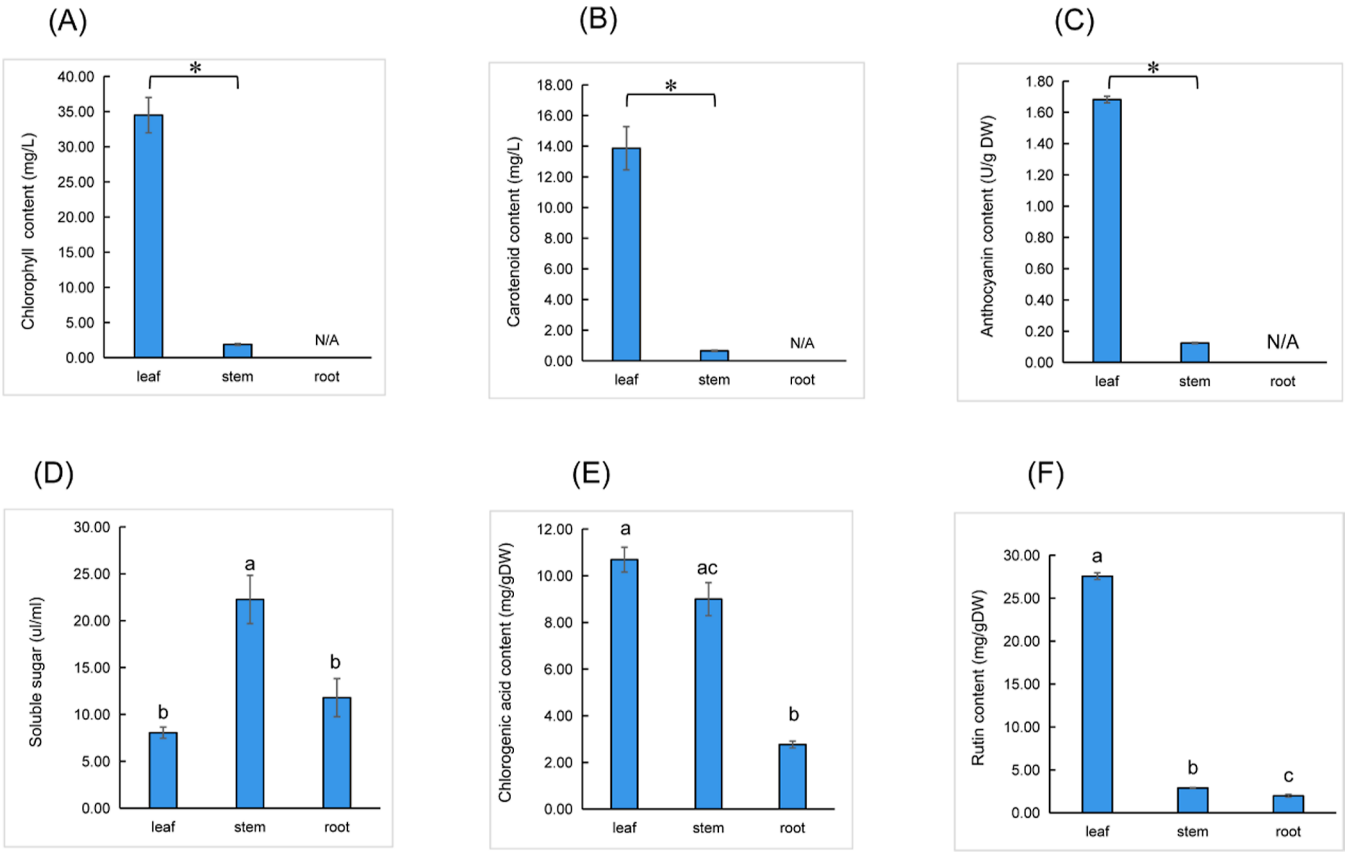

Figure 1. Physiological analyses of leaves, stems, and roots of tobacco. (A) Chlorophyll content; (B) carotenoid content; (C) anthocyanin content; (D) soluble sugar content; (E) chlorogenic acid content; (F) rutin content. Data are presented as the mean ± standard deviation (SD) from at least three independent biological replicates. Different lowercase letters or "*" denote significant differences ($P < 0.05$). N/A denotes no detection in the roots.

development of tobacco, and the transcriptional dynamics of genes related to cytokinin and jasmonic acid biosynthesis and signaling pathways have greatly expanded the understanding of the dynamic regulatory network of plant leaf development.[16]

Therefore, in this study, we applied label-free proteomics technology and untargeted liquid chromatography and mass spectrometry-based metabolomics technology to study the leaves, stems, and roots of seedling tobacco. To obtain new clues about the early biosynthesis mechanism and distribution characteristics of tobacco aroma precursors, as well as other important compounds, 4992 proteins and 298 metabolites were obtained.

2. RESULTS

2.1. Index Differences in the Leaves, Stems, and Roots of Tobacco. We first analyzed the differences in the contents of some aroma precursors of tobacco organs (Table S1). Figure 1A–C suggested that the contents of plastid pigments (chlorophyll and carotenoid) and anthocyanins were lower in stems than in leaves, and these compounds were not detected in tobacco seedling roots. The soluble sugar content in freeze-dried tobacco seedling stems was the highest (Figure 1D). The contents of the polyphenols chlorogenic acid and rutin in different organs were measured, and the results showed that the chlorogenic acid content was higher in the leaf and stem groups than in the root group (Figure 1E). Rutin had a high content in the leaf group, but the rutin content in the stem and root groups was very low (Figure 1F).

2.2. Identification and Functional Categories of Proteins. The Proteome Discoverer (PD) software data analysis results showed that this study had good sample repeatability (Figure S1). A total of 4992 proteins were identified in roots, stems, and leaves, which contained 2182 significantly differentially expressed proteins (Table S2 and Figure 2B). KOBAS 3.0 online software was used to process KEGG pathways. Figure 2C shows the top 20 enriched pathways of the differentially expressed proteins. The carbon fixation in the photosynthetic organism pathway, glycolysis pathway, biosynthesis of the amino acid pathway, pentose phosphate pathway, and starch and sucrose metabolism pathway was significantly enriched. MapMan bin codes and GO terms were used to process the functional classification of differential proteins. Figure 3 showed the top five functional classifications of significantly differentially expressed proteins among the different organ groups. They were protein folding and protein activation, stress, photosynthesis, RNA transcription and binding, and secondary metabolism. Figure S2 showed that GO term classification was involved in protein folding and glycolytic process (BP), cytoplasm and cytosol (CC), and unfolded protein binding and ATP binding (MF).

2.3. Protein–Protein Interaction (PPI) Analysis of Differentially Expressed Proteins. Protein–protein interaction networks of the proteins were obtained using open-access STRING software. A total of 1577 nodes connected by 1519 interactions in significantly changed proteins were found. Cluster network analysis in STRING software showed that

https://doi.org/10.1021/acsomega.2c03877
ACS Omega 2022, 7, 33295–33306

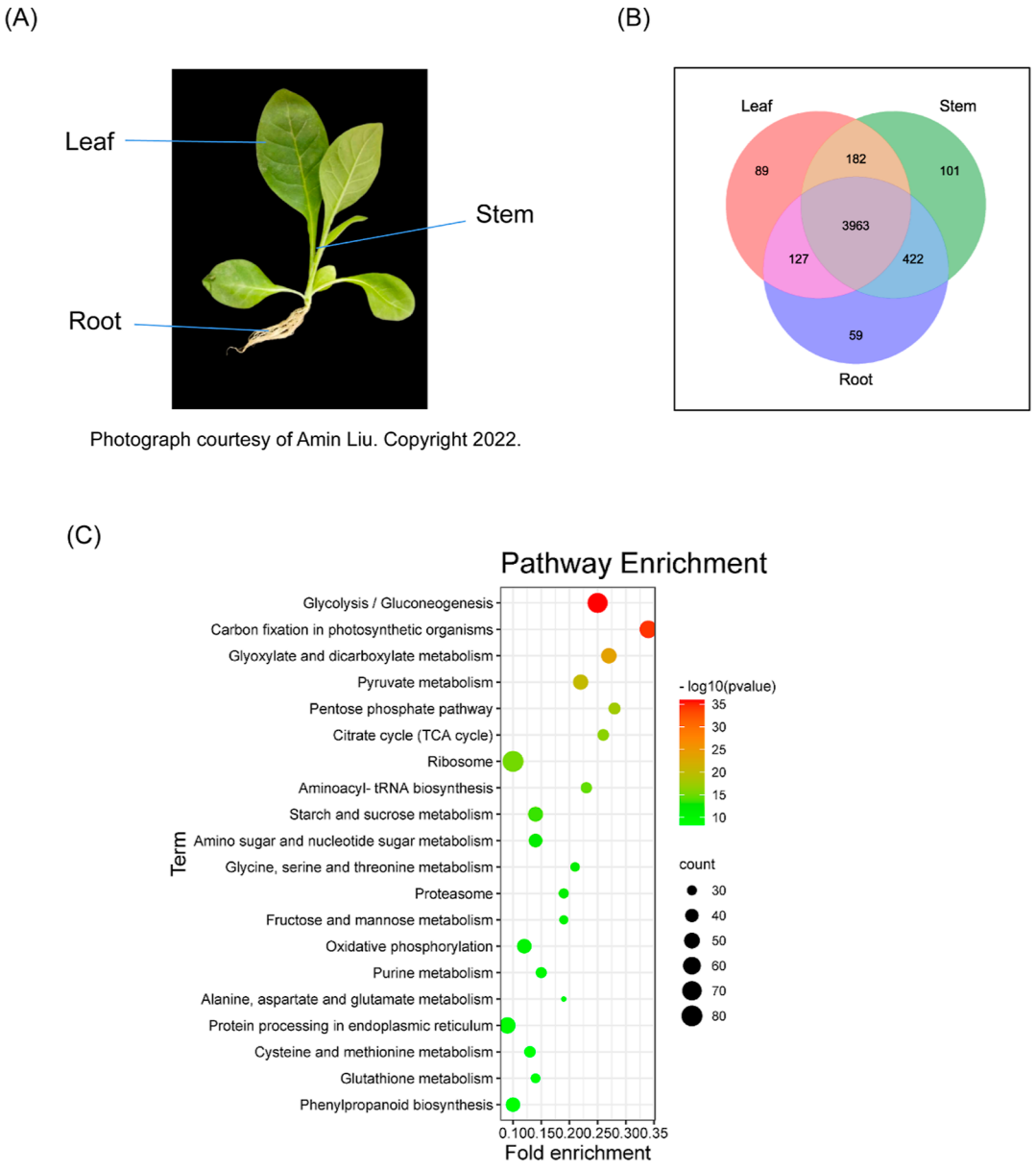

Figure 2. Multivariate data analysis from proteomics. (A) Morphological traits of Yun 87 tobacco seedlings; (B) Venn diagram showing the number of identified proteins in each group of leaves, stems, and roots. (C) KEGG pathway enrichment result of differential proteins.

most compacts were constituted by significantly changed proteins involved in protein processing in the endoplasmic reticulum; oxidative phosphorylation; ribosome, amino sugar, and nucleotide sugar metabolism; aminoacyl-tRNA biosynthesis; glutathione metabolism; glyoxylate and dicarboxylate metabolism; alanine, aspartate, and glutamate metabolism; glycolysis/gluconeogenesis; and carbon fixation in photosynthetic organism pathways (Figure S3).

2.4. Identification and Analysis of Metabolites. The Compound Discoverer 3.2 (CD) software was used for database search analysis of metabolomics mass spectral data, and then MetaboAnalyst was used for data analysis of the obtained metabolites. A total of 298 metabolites were obtained (Table S2), and the principal component analysis (PCA) results of the metabolites are shown in Figure 4A. The 197 differential metabolites obtained were classified by the PubChem database, and the results showed that most of the differential metabolites were amino acids, organic acids, fatty acids, and alkaloids (Figure 4B). The hierarchical clustering analysis tree (Figure S4A) was shown by MetaboAnalyst software analysis. Pathway enrichment analysis of these differential metabolites was also conducted, which showed that beta-alanine metabolism; isoquinoline alkaloid biosynthesis; alanine, aspartate, and glutamate metabolism; aminoacyl-tRNA biosynthesis; arginine biosynthesis; nicotinate and nicotinamide metabolism; linoleic acid metabolism; biosynthesis of secondary metabolites—unclassified; tyrosine metabolism; and butanoate metabolism were the top 10 enriched pathways of differential metabolites (Figure S4B). Additionally, our correlation analysis results showed that scopoletin, nornicotine, myosmine, anatalline, and anatabine had a significantly positive correlation with DL-phenylalanine, L-(+)-leucine, L-histidine, L-tyrosine, and valine, respectively. A positive correlation of nechlorogenic acid and rutin with DL-arginine and L-aspartic acid, respectively, was observed; however, (S)-nicotine showed a significantly negative correlation with the presence of tyrosine (Figure S5).

https://doi.org/10.1021/acsomega.2c03877
ACS Omega 2022, 7, 33295−33306

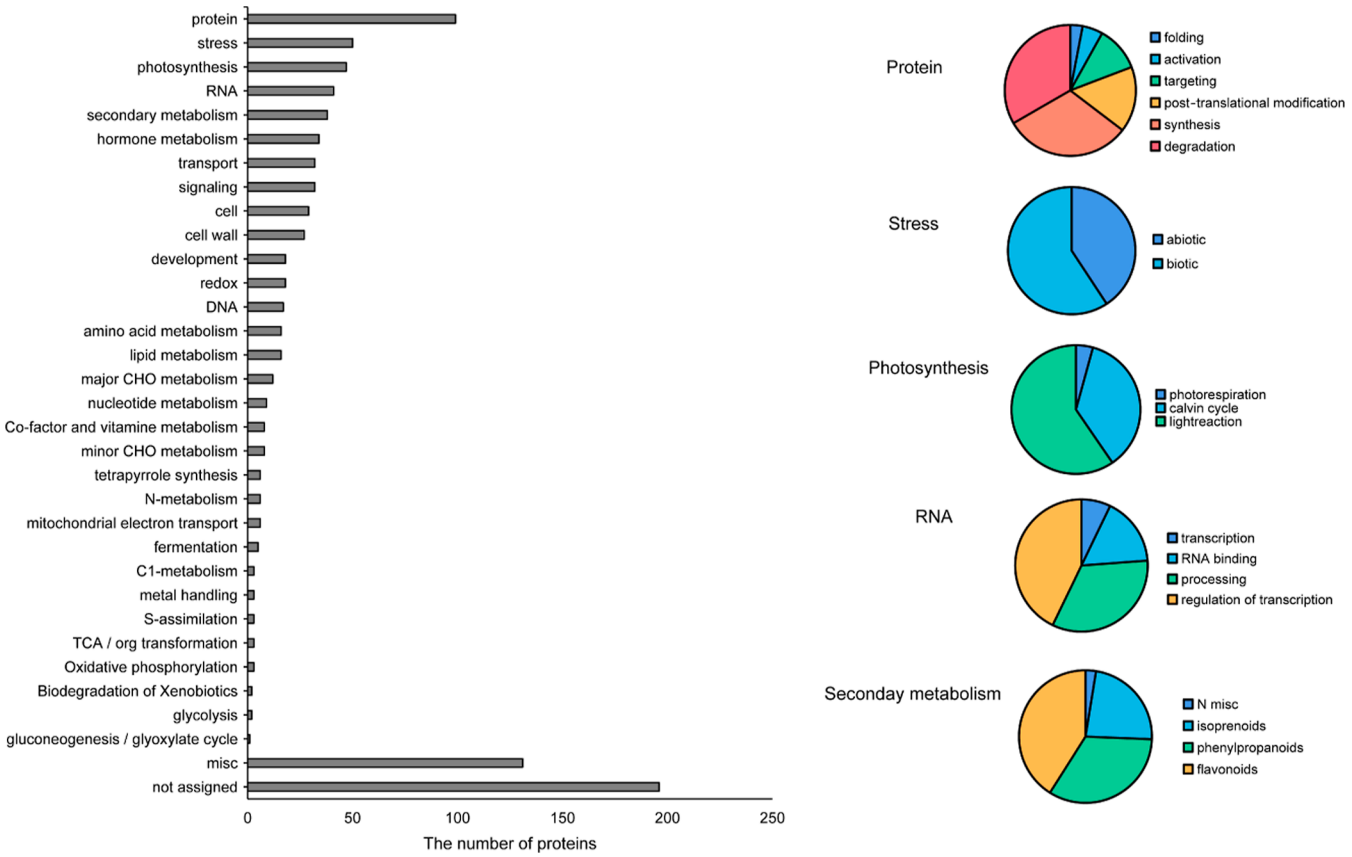

Figure 3. Functional category analysis of differentially expressed proteins. MapMan bin codes were used to process the functional classification of differential proteins.

2.5. Combined Pathway Analysis of Differentially Expressed Proteins and Metabolites. The KEGG accessions of differential proteins and metabolites were submitted for KEGG pathway mapper analysis. Pathway analysis diagrams were drawn for the starch and sucrose metabolism pathways (Figure 5) with PYG, glycogen phosphorylase; malZ, alpha-glucosidase; SUS, sucrose synthase; AMY, alpha-amylase; E3.2.1.2, beta-amylase; GN5_6, glucan endo-1,3-beta-glucosidase 5/6; glgA, starch synthase; UGP2, UTP--glucose-1-phosphate uridylyltransferase; GN1_2_3, glucan endo-1,3-beta-glucosidase 1/2/3; and WAXY, granule-bound starch synthase, being significantly highly expressed in the stem group. HK, hexokinase; TPS, trehalose 6-phosphate synthase/phosphatase; GBE1, 1,4-alpha-glucan branching enzyme; E2.7.1.4, fructokinase; INV, beta-fructofuranosidase; bglX, beta-glucosidase; Pgm, phosphoglucomutase; and glgC, glucose-1-phosphate adenylyltransferase had the highest expression levels in the leaves. Carbon fixation in photosynthetic organisms, glycolysis, biosynthesis of amino acids, and the pentose phosphate pathway were also shown in Figure 6. After enrichment analysis of all of these proteins involved in carbohydrate metabolism and energy metabolism pathways, we found that carbohydrate metabolism and energy metabolism were more active in the stems and leaves of tobacco seedlings than in the roots.

In addition, the different abundances of amino acids involved in the differential metabolites in leaves, stems, and roots were also well demonstrated, such as the synthesis of histidine, valine, and leucine being significantly increased compared with the root and leaf groups; the content of tyrosine and aspartic acid being significantly decreased compared with those in the stems and leaves; and the contents of histidine, valine, leucine, tyrosine, and aspartic acid being significantly decreased compared with those in the stems and roots.

2.6. There Are Organ Differences in Flavonoid and Alkaloid Secondary Metabolism in Seedling-Period Tobacco. The results of MapMan bin code analysis showed that there were differences in the overall secondary metabolism of tobacco leaves, stems, and roots at the seedling stage, especially in the expression of phenylpropanoid-, flavonoid-, and alkaloid-related proteins (Figure 7A). We performed a cluster analysis of differential proteins related to flavonoid and alkaloid biosynthesis by heat map (Figure 7B,C). Combined with the metabolomics identification results of some key aroma precursor substances in tobacco, we highlighted the differences in the abundance of some flavonoids and alkaloid metabolites in a bar chart in Figure 8.

3. DISCUSSION

3.1. Contents of Some Aroma Precursors Were Different in the Leaves, Stems, and Roots of Tobacco at the Seedling Stage. Since tobacco is an important commercial economic crop, its quality, especially aroma products, greatly impacts business economic benefits. The aroma precursors of tobacco leaves are the material basis of the tobacco aroma style, which is closely related to the sensory smoking quality.[17] Aroma precursors of tobacco mainly refered to carbohydrates, carotenoids, polyphenols, alkaloids, and organic acids.[18] Neophytadiene produced by chlorophyll degradation in tobacco leaves was an important terpene

https://doi.org/10.1021/acsomega.2c03877
ACS Omega 2022, 7, 33295−33306

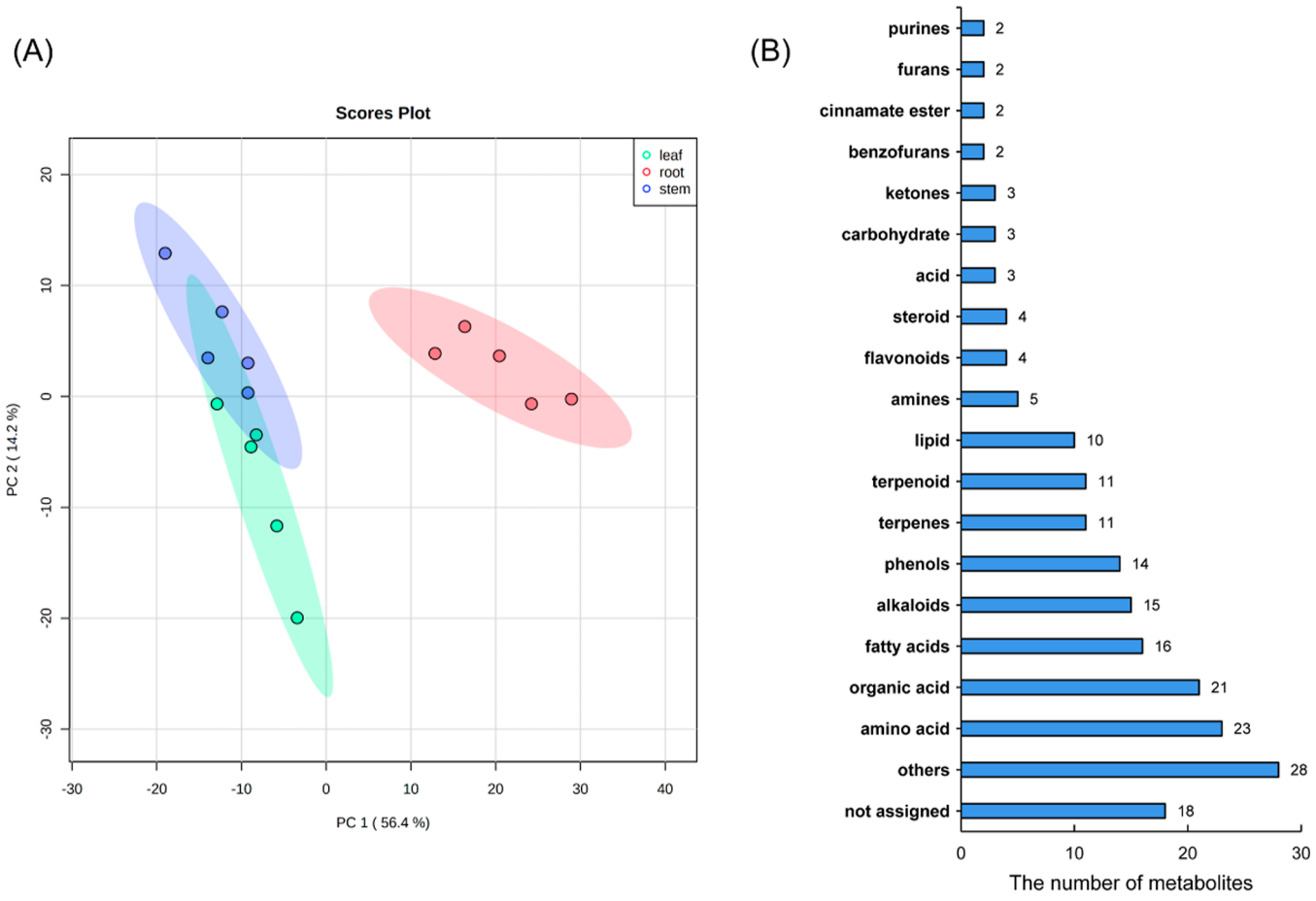

Figure 4. Protein identification in the leaves, stems, and roots of tobacco. (A) PCA was used to analyze the differences within and among experimental groups. PCA score plots from different organs; (B) the bar diagram shows the category results of the differential metabolites.

compound in tobacco leaves and the component with the largest content in neutral volatile aroma substances of flue-cured tobacco, as well as megastigmatrienone, and beta-damascone, the degradation product of carotenoids, which was also an important aroma-producing component in tobacco leaves.[19] As shown in Figure 1A−C, tobacco leaves at the seedling stage contained high levels of chlorophyll, carotenoids, and anthocyanins, while the pigment content in stems was relatively low.

The content of total soluble sugars in tobacco leaves also had varying degrees of influence on the sweetness and flavor of tobacco aroma.[20] However, the detection results of sugar in Figure 1D showed that the soluble sugar content in the seedling tobacco stem group was higher. This result may be related to the organ characteristics of material transport and the main photosynthetic sites and energy storage organs of higher plants.[21]

Secondary metabolites of polyphenols are not only involved in the growth, development, and metabolism of tobacco but also important for the color, aroma, and taste of tobacco leaf products.[22] Polyphenols in tobacco mainly included chlorogenic acid and rutin.[23] Our physiological measurements showed that the contents of chlorogenic acid and rutin were high in tobacco leaves and a small amount in the roots, which was consistent with reports that chlorogenic acid and rutin were synthesized mainly in plant leaves and then transported to other organs.

3.2. Organ Location Differences Affected the Metabolic Profile of Tobacco in Carbohydrate Metabolism, Energy Metabolism, and Biosynthesis of Amino Acids.

The starch and sucrose metabolism pathway, glycolysis, pentose phosphate pathway, and carbon fixation in photosynthetic organs are also the main pathways of carbohydrate and energy metabolism in plants. High-sugar tobacco is usually the first choice of tobacco producers and consumers because the preference for tobacco products is proportional to the level of sugar.[24] In the starch and sucrose metabolism pathway, sucrose metabolism was directly controlled by sucrose phosphate synthase (E2.4.1.14/SPS), SUS, and INV. SPS was the main enzyme involved in sucrose synthesis, and it catalyzed the synthesis of UDP-glucose and fructose-6-phosphate into sucrose 6-phosphate. SUS catalyzed both sucrose synthesis and hydrolysis, and INV in vacuoles was involved in sucrose hydrolysis.[25] In the presence of UDP, SUS reversibly converts sucrose to UDP-glucose, and amylose was then formed under the catalysis of WAXY. Furthermore, GBE1 directly controlled starch production, and AMY catalyzes starch degradation to release considerable amounts of maltose.[26] The relatively high expression of these key enzymes in starch and sucrose metabolism in tobacco stems and leaves at the seedling stage led us to hypothesize that it contributed to the highest sugar accumulation in tobacco seedling stems.

In our study, the carbon fixation in the photosynthetic organ pathway was the most significantly enriched pathway of differential proteins. From the result of heat-map clustering of differential proteins involved in this pathway, it was found that the expression level of these proteins in leaves and stems was the

https://doi.org/10.1021/acsomega.2c03877
ACS Omega 2022, 7, 33295−33306

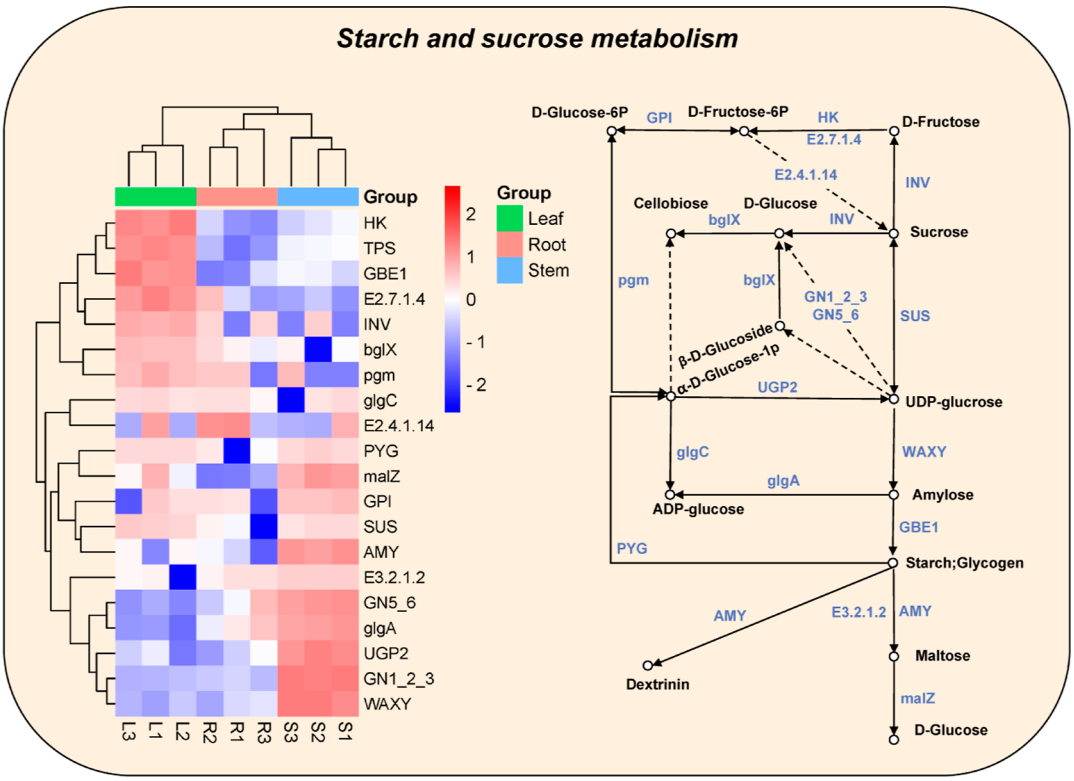

Figure 5. Changes in starch and sucrose metabolism. The pathways were drawn based on the KEGG database. PYG, glycogen phosphorylase [EC:2.4.1.1]; SUS, sucrose synthase [EC:2.4.1.13]; E2.4.1.14, sucrose phosphate synthase [EC:2.4.1.14]; GBE1, 1,4-alpha-glucan branching enzyme [EC:2.4.1.18]; glgA, starch synthase [EC:2.4.1.21]; HK, hexokinase [EC:2.7.1.1]; E2.7.1.4, fructokinase [EC:2.7.1.4]; UGP2, UTP--glucose-1-phosphate uridylyltransferase [EC:2.7.7.9]; glgC, glucose-1-phosphate adenyltransferase [EC:2.7.7.27]; AMY, alpha-amylase [EC:3.2.1.1]; E3.2.1.2, beta-amylase [EC:3.2.1.2]; malZ, alpha-glucosidase [EC:3.2.1.20]; INV, beta-fructofuranosidase [EC:3.2.1.26]; GPI, glucose-6-phosphate isomerase [EC:5.3.1.9]; Pgm, phosphoglucomutase [EC:5.4.2.2]; bglX, beta-glucosidase [EC:3.2.1.21]; WAXY, granule-bound starch synthase [EC:2.4.1.242]; TPS, trehalose 6-phosphate synthase/phosphatase [EC:2.4.1.15 3.1.3.12]; GN1_2_3, glucan endo-1,3-beta-glucosidase 1/2/3 [EC:3.2.1.39]; and GN5_6, glucan endo-1,3-beta-glucosidase 5/6 [EC:3.2.1.39].

highest. The results showed that photosynthetic carbon fixation activity was more active in the stems and leaves of tobacco during the seedling stage, which was closely related to the leaf and stem as the main sites of photosynthesis. In addition to providing energy, the pentose phosphate pathway mainly provided various raw materials for anabolism, such as providing NADPH for fatty acid biosynthesis, providing 5-phosphate ribose for nucleotide coenzyme and nucleotide synthesis, and providing erythritose 4-phosphate for the synthesis of aromatic amino acids. The C4, C5, and C7 compounds, transketoenzyme, and transaldoenzyme produced by this pathway were also related to photosynthesis. Therefore, the pentose phosphate pathway is an important multifunctional metabolic pathway. Glucose-6-phosphate 1-dehydrogenase (O65856), a key enzyme in the pentose phosphate pathway identified in our study, was also highly expressed in leaves and stems, followed by roots. Glycolysis can use glucose to produce pyruvate and ATP, and then pyruvate in the presence of oxygen enters the tricarboxylic acid cycle and participates in amino acid biosynthesis and metabolism and fatty acid metabolism. PK was identified as a key enzyme in the glycolysis pathway, and IDH1 was identified as a key enzyme in the tricarboxylic acid (TCA) cycle, both of which are characterized by differential expression in organs.

Free amino acids are precursors of the Maillard reaction, and the aroma of flue-cured tobacco is an important material foundation for the later tobacco flavor contribution that cannot be underestimated. The metabolomic result (Figure 4B) also showed abundant amino acid species with it ranked number 1 in the statistical table of differential metabolite classification results, and pathway enrichment analysis of differential metabolites (Figure S4B) showed that alanine, aspartate, and glutamate metabolism, arginine biosynthesis, and tyrosine metabolism pathways were greatly enriched. Then, we mapped the partially significantly differentially abundant amino acid metabolites into KEGG pathways and generated Figure 6. In this pathway, the synthesis of histidine, tyrosine, phenylalanine, valine, and leucine was significantly increased in the root group compared with the leaf and stem groups. However, the contents of aspartic acid and proline were significantly increased in the leaf group compared with the stem and root groups. Amino acids were the synthetic components of many proteins and the precursors of most alkaloids.[27] Therefore, the organ differences of these amino acid metabolites also laid a foundation for the identification of differential proteins in the early stage of this study and the subsequent secondary metabolic analysis.

3.3. Organ Location Differences Affected the Metabolic Profile of Tobacco in the Biosynthesis of Secondary Metabolites. MapMan bin code analysis showed that the protein expression in secondary metabolism, especially in phenylpropanoid, flavonoid, and alkaloid biosynthesis, was different in the leaf, stem, and root groups of tobacco seedlings.

From the phenylpropanoid biosynthesis pathway, 20% of the secondary metabolites in plants were derived.[28,29] Flavonoids

https://doi.org/10.1021/acsomega.2c03877
ACS Omega 2022, 7, 33295−33306

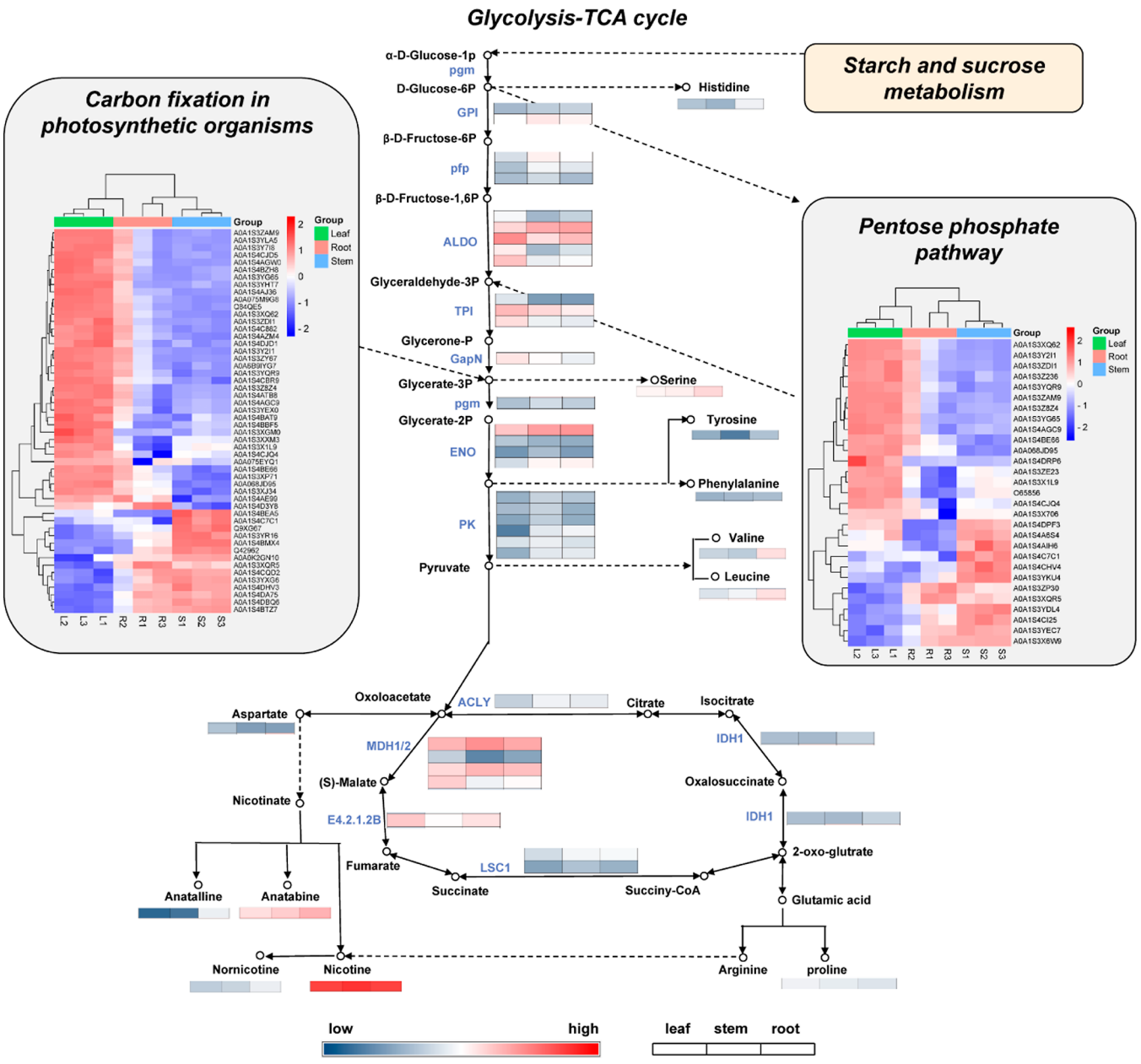

Figure 6. Changes in proteins and metabolites in carbon fixation in photosynthetic organisms, glycolysis, and the pentose phosphate pathway. The pathways were drawn based on the KEGG database. GapN, glyceraldehyde-3-phosphate dehydrogenase (NADP+) [EC:1.2.1.9]; PK, pyruvate kinase [EC:2.7.1.40]; Pfp, diphosphate-dependent phosphofructokinase [EC:2.7.1.90]; ALDO, fructose-bisphosphate aldolase, class I [EC:4.1.2.13]; ENO, enolase [EC:4.2.1.11]; TPI, triosephosphate isomerase (TIM) [EC:5.3.1.1]; GPI, glucose-6-phosphate isomerase [EC:5.3.1.9]; Pgm, phosphoglucomutase [EC:5.4.2.2]; MDH1, malate dehydrogenase [EC:1.1.1.37]; MDH2, malate dehydrogenase [EC:1.1.1.37]; IDH1, isocitrate dehydrogenase [EC:1.1.1.42]; ACLY, ATP citrate (pro-S)-lyase [EC:2.3.3.8]; E4.2.1.2B, fumarate hydratase, class II [EC:4.2.1.2]; LSC1; succinyl-CoA synthetase alpha subunit [EC:6.2.1.4 6.2.1.5].

are major secondary metabolites derived from the plant phenylpropanoid pathway that play important roles in plant development.[30] In our study, we identified cinnamyl-alcohol dehydrogenase (CAD), peroxidase (POD), caffeic acid 3-*O*-methyltransferase/acetylserotonin *O*-methyltransferase (COMT), phenylalanine ammonia-lyase (PAL), 4-coumarate--CoA ligase (4CL), 5-*O*-(4-coumaroyl)-D-quinate 3′-monooxygenase (CYP98A), and caffeoyl-CoA *O*-methyltransferase (E2.1.1.104), the key enzymes in the biosynthesis of phenylpropanoids and flavonoids, which had the highest expression levels in the roots of tobacco seedlings. However, feruloyl CoA ortho-hydroxylase 2-like (F6H) and shikimate *O*-hydroxycinnamoyltransferase (E2.3.1.133) had higher expression levels in the leaf and stem groups. Under the action of these key enzymes with organ differences, our metabolome identified the key aroma precursors, flavonoid metabolites rutin, (+)-gallocatechin, and sophoraflavanone G, as well as neochlorogenic acid, with the highest abundance in leaves. Scopoletin and procyanidin A2, however, were higher in roots. Among them, the different abundance trends of rutin and neochlorogenic acid in organs were consistent with the different content trends of rutin and chlorogenic acid in leaves, stems, and roots determined at the initial stage.

https://doi.org/10.1021/acsomega.2c03877
ACS Omega 2022, 7, 33295−33306

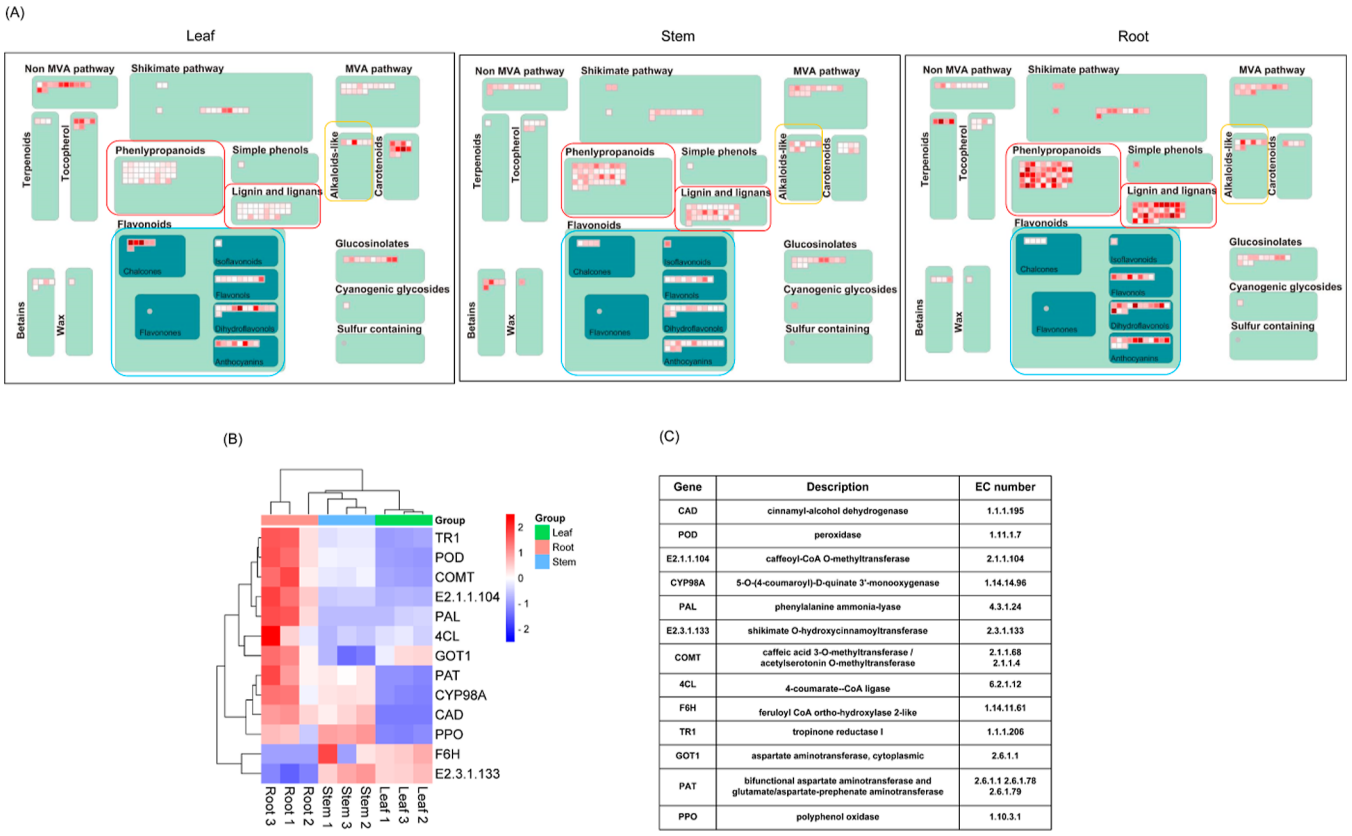

Gene	Description	EC number
CAD	cinnamyl-alcohol dehydrogenase	1.1.1.195
POD	peroxidase	1.11.1.7
E2.1.1.104	caffeoyl-CoA O-methyltransferase	2.1.1.104
CYP98A	5-O-(4-coumaroyl)-D-quinate 3'-monooxygenase	1.14.14.96
PAL	phenylalanine ammonia-lyase	4.3.1.24
E2.3.1.133	shikimate O-hydroxycinnamoyltransferase	2.3.1.133
COMT	caffeic acid 3-O-methyltransferase / acetylserotonin O-methyltransferase	2.1.1.68 2.1.1.4
4CL	4-coumarate--CoA ligase	6.2.1.12
F6H	feruloyl CoA ortho-hydroxylase 2-like	1.14.11.61
TR1	tropinone reductase I	1.1.1.206
GOT1	aspartate aminotransferase, cytoplasmic	2.6.1.1
PAT	bifunctional aspartate aminotransferase and glutamate/aspartate-prephenate aminotransferase	2.6.1.1 2.6.1.78 2.6.1.79
PPO	polyphenol oxidase	1.10.3.1

Figure 7. Differential analysis of secondary metabolism in tobacco leaf stems and roots at the seedling stage. (A) Secondary metabolism analysis of leaves, stems, and roots in tobacco seedlings by MapMan bin codes; (B) cluster analysis of differential proteins related to phenylpropanoid, flavonoid, and alkaloid biosynthesis as shown in a heat map. (C) Table of differential proteins related to phenylpropanoid, flavonoid, and alkaloid biosynthesis.

In this study, differential proteins and differential metabolites were enriched in pathways involving alkaloid biosynthesis. tropinone reductase I (TR1), aspartate aminotransferase (GOT1), bifunctional aspartate aminotransferase (PAT), and glutamate/aspartate-prephenate aminotransferase are involved in tropane, piperidine, and pyridine alkaloid biosynthesis, and polyphenol oxidase (PPO) is involved in isoquinoline alkaloid biosynthesis. Then, we constructed a bar chart of the alkaloid metabolites, which indicated the differences in the synthesis of metabolites involved in the alkaloid biosynthesis pathway in leaves, stems, and roots. Nicotinamide was involved in the biosynthesis of pyridine alkaloids in KEGG pathways, such as nicotine, nornicotine, anatabine, and anatalline biosynthesis. Our untargeted metabolomic identification results showed that the nicotine content in the seedling tobacco leaves and stems was higher, while nornicotine, anatabine, and anatalline in the tobacco seedling stage had the highest content in the root group, followed by the stem group and the leaf group. The reason might be that nicotine and other pyridine alkaloids were mainly synthesized in tobacco roots and subsequently transferred to leaves and other aerial plant parts through the xylem.[9,31,32] In addition, our metabolite identification results also found a minor tobacco alkaloid, myosmine, which was structurally related to nicotine,[33] and actinidine. It was an unusual monoterpene alkaloid commonly found in the kiwifruit family and the Valerianaceae family plant,[34] and the contents was the highest in the root group. Laurolitsine, an aporphine alkaloid;[35] tetramethylpyrazine, a pyrazine alkaloid;[36] and valeroidine, a tropane alkaloid and arecoline, were also found in tobacco seedlings, and they all had the highest identification level in the tobacco seedling root group. The organ difference characteristics of these alkaloid metabolites are interestingly consistent. This result provides new verification of the synthesis and distribution difference in alkaloids, one of the key aroma precursors in tobacco at the seedling stage.

4. CONCLUSIONS

In this study, proteomic and metabolomic analyses were carried out on different organs (leaf, stem, and root) of Yunyan 87 tobacco seedlings, and a total of 2182 significantly different proteins and 298 metabolites were obtained. With the help of KEGG pathway enrichment, MapMan bin codes, MetaboAnalyst online software, and other analysis tools, it was concluded that the differences in proteins and metabolites in seedling tobacco leaves, stems, and roots mainly involve carbohydrate metabolism; energy metabolism; amino acid biosynthesis; and phenylpropanoid, flavonoid, and alkaloid synthesis pathways. In particular, it was also found that the contents of secondary metabolite alkaloids, such as nornicotine, anatabine, anatalline, and myosmine, were significantly higher in tobacco roots than in leaves and stems at the seedling stage. This study provided a mapping for a better understanding of the underlying metabolic mechanism differences of leaves, stems, and roots in the seedling stage of tobacco. It also provides a research basis for further exploring the synthesis of aroma precursor substances in tobacco leaves. At the same time, it has some reference value for organ-specific studies in other plants.

https://doi.org/10.1021/acsomega.2c03877
ACS Omega 2022, 7, 33295−33306

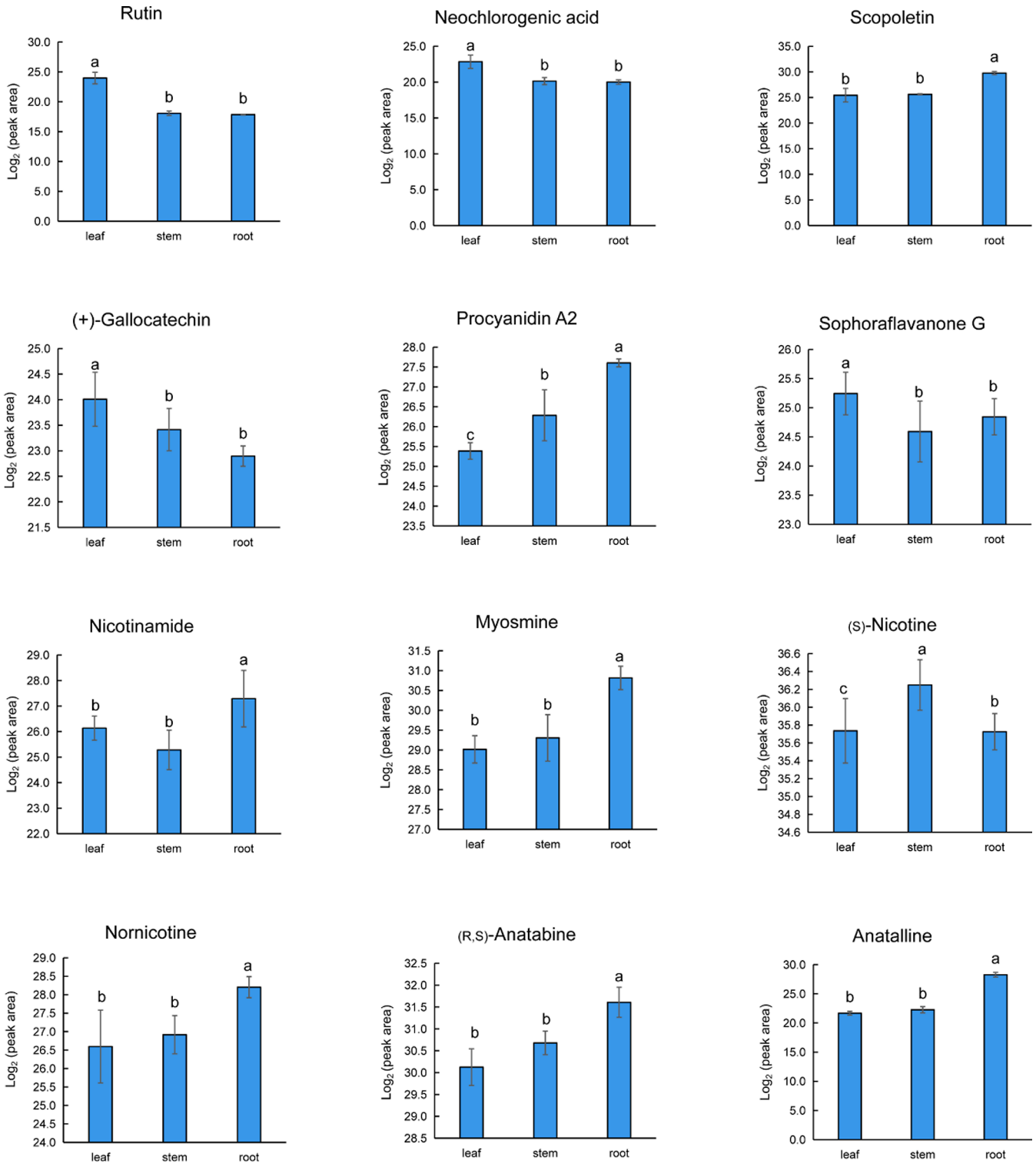

Figure 8. Analysis of some metabolites related to secondary metabolism. Typical change patterns of representative compounds in tobacco organs. Columns with different letters (a, b, or c) indicate that there is a significant difference between the two groups ($p < 0.05$).

5. MATERIALS AND METHODS

5.1. Plant Materials. In China, Yunyan 87 is recognized as a flue-cured tobacco variety and has been widely studied due to its excellent product quality characteristics.[37] Therefore, the tobacco variety Yunyan 87 was provided by Anhui Wannan Tobacco Co., Ltd. (Anhui, China) and grown in a greenhouse. Tobacco seedling cultivation was performed in a nursery shed at a temperature of 28 °C and a humidity of approximately 75%. Leaves, stems, and roots from each group were collected from 60-day-old *N. tabacum* seedlings for all the experimental analyses, flash-frozen in liquid nitrogen, and then stored at −80 °C for subsequent analysis.

5.2. Determination of the Aroma Precursor Index. We referred to the method of Wellburn and Lichtenthaler to determine the contents of chlorophyll a (Chl a), chlorophyll b

https://doi.org/10.1021/acsomega.2c03877
ACS Omega 2022, 7, 33295−33306

(Chl b), and carotenoids (Car).[38] Total anthocyanins were extracted as described by Neff and Chory,[39] and then anthocyanins were determined by measuring the A530 and A657 of the aqueous phase and expressed in (A657−A530) per dry weight (DW). The soluble sugar content was measured using a kit (Nanjingjiancheng, Jiangsu, China). Chlorogenic acid (CGA) extraction and content determination were performed in accordance with the methods described by Kong et al.[40] Rutin was extracted according to the methods of Ganzera et al.,[41] and the UV absorbance was monitored at 284 nm.

5.3. Protein Extraction, Purification, and Enzymolysis. The protein extraction process was conducted according to Carpentier et al. with slight modification.[42] Fresh materials (50 mg) were ground in liquid nitrogen and then resuspended in 5 mL of ice-cold extraction buffer. Then, 5 mL of ice-cold Tris-phenol (pH > 7.8) was added, and the sample was mixed for 15 min at 4 °C. After centrifugation (6000*g*, 3 min, 4 °C), the phenolic phase was collected and precipitated overnight with five volumes of 100 mM ammonium acetate in methanol at −20 °C. After precipitation, the pellet was rinsed twice in ice-cold acetone. The pellet was air-dried and resuspended in 100 μL of lysis buffer (7 M urea, 2 M thiourea, 4% CHAPS, 2 mM EDTA, 10 mM DTT, and 1 mM PMSF). The protein concentration was determined by the Bradford method with bovine serum albumin as the standard. Protein purification and enzymolysis were performed in accordance with the methods described by Zhu et al.[43] Peptides were desalted with a ZipTip column (Millipore Sigma, Temecula, CA, USA).

5.4. Protein Analysis Using Nano LC−MS/MS. Protein analysis using nano LC−MS/MS was performed in accordance with the methods described by Zhu et al.[43] The tryptic peptides were analyzed on an Easy-nLC 1000 system coupled with an Orbitrap Exploris 480 mass spectrometer (Thermo Scientific Inc., San Jose, CA, USA). Peptides in 0.1% formic acid were loaded onto an Acclaim Pep Map 100 C18 column (250 mm × 75 μm, 2 μm-C18) (Thermo Scientific Inc., San Jose, CA, USA). Mobile phase A was ddH_2O, mobile phase B was 80% acetonitrile, and the following linear gradient was applied: 0−1 min, 3% B to 8% B; 1−102 min, 8% B to 45% B; 102−106 min, 45% B to 95% B; and 106−115 min, 95% B. The flow rate was 300 nL min^{-1}. The eluted peptides were ionized by a nanoelectrospray flex source and analyzed in data-dependent acquisition mode with Thermo Xcalibur software. Full-scan mass spectra were acquired in the MS over 350−1500 m/z with a resolution of 60,000. The 10 most intense precursor ions were selected for collision-induced (CID) fragmentation in the linear ion trap at a normalized collision energy of 30%. The MS2 ions were detected using a normal ion trap scan rate.

5.5. Protein Identification. The raw data were analyzed within PD (version 2.4, Thermo Scientific). Identified proteins were searched against the UniProtKB database (*N. tabacum*, 77079 entries, downloaded 2021.05.21). The mass tolerance values of MS and MS/MS were set to 10 ppm and 0.2 Da, respectively. The enzyme digestion method was set as trypsin. Peptides with fewer than two unique peptides were excluded from further analysis.

5.6. Proteomic Bioinformatic Analysis. KOBAS 3.0 online software was used to perform KEGG pathway enrichment analysis and GO enrichment analysis. The Kyoto Encyclopedia of Genes and Genomes (KEGG) database (http://www.kegg.jp/) was used to annotate protein and metabolite pathways. MapMan bin codes were used to process protein functional classification and protein pathway mapping. Proteins were classified into molecular function, cellular component, and biological process categories by GO terms. The protein−protein interactions were analyzed in STRING (Version 11.5). The required confidence score was set as >0.900 for highly confident interactions. A K-means algorithm in STRING clusters the network. The visualization of some data analysis results including Pearson's correlation coefficient analysis was completed using the microbial information platform (http://www.bioinformatics.com.cn).

5.7. Metabolite Extraction and Identification. Metabolite extraction was performed in accordance with the methods described by Zhu et al. with five independent biological replicates.[43] Mass spectrometric analysis of metabolome samples referred to the method of Zhong et al. with some modifications.[44] The metabolite samples were analyzed on an UHPLC system (Thermo Scientific) coupled with a Thermo Scientific Orbitrap Exploris 480 mass spectrometer. The separation of all samples was performed on a BEH C18 column (Thermo Scientific, Accucore C18, 100 mm × 2.1 mm, 1.7 μm) at a column temperature of 45 °C. The flow rate was 0.4 mL min^{-1}, and the mobile phase consisted of 0.1% formic acid aqueous as solvent A and 0.1% formic acid in acetonitrile as solvent B with the following gradient program: 0−0.5 min, 0.1% B; 0.5−21.5 min, 40% B; 21.5−23.5 min, 90% B; and 23.5−25.5 min, 90% B. The mass spectrometer conditions were as follows: 50 arbitrary units (arb) of sheath gas, 10 arb of aux gas, 2.5 arb of sweep gas, 300 °C ion transfer tube temperature, 350 °C vaporizer temperature, +3500 V positive ion spray voltage, −2500 V negative ion spray voltage, and an MS scan range of 90−900 m/z. Positive- and negative-mode ionization was employed to acquire fragmentation data that were used for identifying metabolites based on database searching. The precursor isolation window was 1.5 Da, and the activation type was high-energy collision-induced dissociation. The Orbitrap resolution for full MS was 60,000, the maximum injection time was 100 msec, and the automatic gain control target was 1,000,000. For the MS/MS experiments, the resolution was 15,000.

5.8. Metabolomic Data Processing and Analysis. We used Compound Discoverer 3.2 (CD) software from Thermo Fisher Scientific to process untargeted metabolomics data. MetaboAnalyst 5.0 online software evaluated sample repeatability by PCA and performed pathway enrichment analysis of differential metabolites. The identified metabolites were classified by the PubChem database (https://pubchem.ncbi.nlm.nih.gov/). We conducted a simple correlation statistical analysis on the contents of amino acids, polyphenols, and nicotine. Then, the results were presented by the Micro-bioinformation platform (http://www.bioinformatics.com.cn).

5.9. Statistical Analysis. Statistical significance was evaluated by 'Student's *t*-test when only two groups were compared or one-way ANOVA, followed by Fisher's test when multiple groups were compared. $P < 0.05$ was considered to be significantly different between groups. All experiments in this study included at least three independent biological replicates.

■ ASSOCIATED CONTENT

Supporting Information

The Supporting Information is available free of charge at https://pubs.acs.org/doi/10.1021/acsomega.2c03877.

PCA and correlation analysis of proteomics; PCA result of proteomics; sample correlation analysis of proteomics;

https://doi.org/10.1021/acsomega.2c03877
ACS Omega 2022, 7, 33295−33306

result of GO functional classification of differential proteins; PPI analysis of significantly differential proteins; five clusters obtained; the main functional classification of each cluster; phylogenetic tree and pathway enrichment analysis of differential metabolites; phylogenetic tree of differential metabolites; pathway enrichment analysis of differential metabolites; correlation analysis of some amino acids, polyphenols, and alkaloids; aroma precursor index analyses of the leaves, stems, and roots of tobacco; metabolite identification of seedling tobacco leaves, stems, and roots; and differentially expressed proteins identification of seedling tobacco leaves, stems, and roots (PDF)

Accession Codes

Accession code: The mass spectrometry proteomics data have been deposited to the ProteomeXchange Consortium via the PRIDE partner repository with the dataset identifier PXD032082. The mass spectrometry metabolomics data can be accessed by https://doi.org/10.5281/zenodo.5804184.

AUTHOR INFORMATION

Corresponding Authors

Wei Zhu − *The Cancer Hospital of the University of Chinese Academy of Sciences (Zhejiang Cancer Hospital), Institute of Basic Medicine and Cancer (IBMC), Chinese Academy of Sciences, Hangzhou 310002, PR China*; orcid.org/0000-0001-9582-3787; Email: zhuwei@ibmc.ac.cn

He Ye − *Department of Pharmacy, Zhejiang Hospital, Hangzhou 310013, PR China*; Email: yehe20092009@163.com

Authors

Amin Liu − *College of Biomedical Engineering & Instrument Science, Zhejiang University, Hangzhou 310027, PR China*

Kailong Yuan − *China Tobacco Zhejiang Industrial Company Limited, Hangzhou 310008, PR China*

Haiqing Xu − *Anhui Wannan Tobacco Company Limited, Xuancheng 242000, PR China*

Yonggang Zhang − *China Tobacco Zhejiang Industrial Company Limited, Hangzhou 310008, PR China*

Jingkui Tian − *The Cancer Hospital of the University of Chinese Academy of Sciences (Zhejiang Cancer Hospital), Institute of Basic Medicine and Cancer (IBMC), Chinese Academy of Sciences, Hangzhou 310002, PR China*

Qi Li − *China Tobacco Zhejiang Industrial Company Limited, Hangzhou 310008, PR China*

Complete contact information is available at: https://pubs.acs.org/10.1021/acsomega.2c03877

Author Contributions

A.L. and K.Y. contributed equally to this work. A.L. and K.Y.: investigation, data curation, writing—original draft, writing—review and editing, visualization. H.X. and Y.Z.: assisting the sampling. J.T. and Q.L.: supervision, resources. W.Z. and H.Y.: project administration.

Notes

The authors declare no competing financial interest.

REFERENCES

(1) Dai, J.; Dong, A.; Xiong, G.; Liu, Y.; Hossain, M. S.; Liu, S.; Gao, N.; Li, S.; Wang, J.; Qiu, D. Production of Highly Active Extracellular Amylase and Cellulase From Bacillus subtilis ZIM3 and a Recombinant Strain With a Potential Application in Tobacco Fermentation. *Front. Microbiol.* **2020**, *11*, 1539.

(2) Banožić, M.; Jokić, S.; Ačkar, D.; Blažić, M.; Šubarić, D. Carbohydrates-Key Players in Tobacco Aroma Formation and Quality Determination. *Molecules* **2020**, *25*, 1734.

(3) Jassbi, A. R.; Zare, S.; Asadollahi, M.; Schuman, M. C. Ecological Roles and Biological Activities of Specialized Metabolites from the GenusNicotiana. *Chem. Rev.* **2017**, *117*, 12227−12280.

(4) Popova, V.; Ivanova, T.; Prokopov, T.; Nikolova, M.; Stoyanova, A.; Zheljazkov, V. D. Carotenoid-Related Volatile Compounds of Tobacco (Nicotiana tabacum L.) Essential Oils. *Molecules* **2019**, *24*, 3446.

(5) Zhang, J. J.; Zhao, C. X.; Chang, Y. W.; Zhao, Y. N.; Li, Q. H.; Lu, X.; Xu, G. W. Analysis of free amino acids in flue-cured tobacco leaves using ultra-high performance liquid chromatography with single quadrupole mass spectrometry. *J. Sep. Sci.* **2013**, *36*, 2868−2877.

(6) Qin, Y.; Bai, S. L.; Li, W. Z.; Sun, T.; Galbraith, D. W.; Yang, Z. F.; Zhou, Y.; Sun, G. L.; Wang, B. W. Transcriptome analysis reveals key genes involved in the regulation of nicotine biosynthesis at early time points after topping in tobacco (Nicotiana tabacum L.). *BMC Plant Biol.* **2020**, *20*, 30.

(7) Zhang, L.; Zhang, X. T.; Ji, H. W.; Wang, W. W.; Liu, J.; Wang, F.; Xie, F. W.; Yu, Y. J.; Qin, Y. Q.; Wang, X. Y. Metabolic profiling of tobacco leaves at different growth stages or different stalk positions by gas chromatography-mass spectrometry. *Ind. Crop. Prod.* **2018**, *116*, 46−55.

(8) Han, Y.; Liu, G. S.; Liu, Y. Y.; Su, X. H.; Zhou, S. M. Study on dynamic changes of aroma components in different growing stages of aromatic tobacco. *Chin. Tobac. Sci.* **2003**, *2*, 41−45.

(9) Dawson, R. F. Accumulation of nicotine in reciprocal grafts of tomato and tobacco. *Am. Bot.* **1942**, *29*, 66−71.

(10) Hidalgo, D.; Martínez-Márquez, A.; Moyano, E.; Bru-Martínez, R.; Corchete, P.; Palazon, J. Bioconversion of stilbenes in genetically engineered root and cell cultures of tobacco. *Sci. Rep.* **2017**, *7*, 45331.

(11) Zhang, K. H.; Zhang, K.; Cao, Y.; Pan, W. P. Co-combustion characteristics and blending optimization of tobacco stem and high-sulfur bituminous coal based on thermogravimetric and mass spectrometry analyses. *Bioresour. Technol.* **2013**, *131*, 325−332.

(12) Li, L.; Wang, R. L.; Jiang, Z. L.; Li, W. W.; Liu, G. Q.; Chen, C. Anaerobic digestion of tobacco stalk: biomethane production performance and kinetic analysis. *Environ. Sci. Pollut. Res.* **2019**, *26*, 14250−14258.

(13) Yan, N.; Zhang, H. B.; Zhang, Z. F.; Shi, J.; Timko, M. P.; Du, Y. M.; Liu, X. M.; Liu, Y. H. Organ- and Growing Stage-Specific Expression of Solanesol Biosynthesis Genes in Nicotiana tabacum Reveals Their Association with Solanesol Content. *Molecules* **2016**, *21*, 1536.

(14) Dai, L. J.; Liu, Y. K.; Zhu, C. W.; Zhong, J. Differential proteomics of tobacco seedling roots at high and low potassium concentrations. *Sci. Rep.* **2021**, *11*, 9194.

(15) Wu, S.; Guo, Y.; Adil, M. F.; Sehar, S.; Cai, B.; Xiang, Z.; Tu, Y.; Zhao, D.; Shamsi, I. H. Comparative Proteomic Analysis by iTRAQ Reveals that Plastid Pigment Metabolism Contributes to Leaf Color Changes in Tobacco (Nicotiana tabacum) during Curing. *Int. J. Mol. Sci.* **2020**, *21*, 2394.

(16) Chang, W.; Zhao, H.; Yu, S.; Yu, J.; Cai, K.; Sun, W.; Liu, X.; Li, X.; Yu, M.; Ali, S.; Zhang, K.; Qu, C.; Lei, B.; Lu, K. Comparative transcriptome and metabolomic profiling reveal the complex mechanisms underlying the developmental dynamics of tobacco leaves. *Genomics* **2020**, *112*, 4009−4022.

(17) Qin, G. J.; Zhao, G. J.; Ouyang, C. B.; Liu, J. L. Aroma components of tobacco powder from different producing areas based on gas chromatography ion mobility spectrometry. *Open Chem.* **2021**, *19*, 442−450.

(18) Chen, J.; Li, Y.; He, X.; Jiao, F. C.; Xu, M. L.; Hu, B. B.; Jin, Y.; Zou, C. M. Influences of different curing methods on chemical compositions in different types of tobaccos. *Ind. Crop. Prod.* **2021**, *167*, 113534.

(19) Wu, Y. J.; Qi, Y.; Zhang, X. Q.; Song, Y. Y.; Xue, G.; Xing, X. X.; Yang, T. Z. Leaf Senescence and Its Relationship with Plastid Pigment Degradation Content and the Degradation Products of Different Varieties of Flue-cured Tobacco. *Acta Agric. Boreali Sin.* **2015**, *5*, 1000−7091.
(20) Roemer, E.; Schorp, M. K.; Piadé, J. J.; Seeman, J. I.; Leyden, D. E.; Haussmann, H. J. Scientific assessment of the use of sugars as cigarette tobacco ingredients: A review of published and other publicly available studies. *Crit. Rev. Toxicol.* **2012**, *42*, 244−278.
(21) Koide, E.; Suetsugu, N.; Iwano, M.; Gotoh, E.; Nomura, Y.; Stolze, S. C.; Nakagami, H.; Kohchi, T.; Nishihama, R. Regulation of Photosynthetic Carbohydrate Metabolism by a Raf-Like Kinase in the Liverwort Marchantia polymorpha. *Plant Cell Physiol.* **2020**, *61*, 631−643.
(22) Gao, Y. B.; Duan, S. J.; Fu, Z. R.; Hu, R. H.; Shi, W. Q.; Cheng, X. Q.; Xiao, R. G.; Ling, P.; Li, Y. C. Research Progress of Polyphenol Content in Tobacco. *J. Anhui Agric. Sci.* **2018**, *46*, 38−40.
(23) Zhuo, W. Z.; Zhang, J. S.; Zou, Y.; Liu, J.; Gao, Z. Y.; Yang, P. P. Determination of Chlorogenic Acid, Scopolamine and Rutin in Tobacco by NIR Combined with Wavelength Screening. *Acta Agric. Jiangxiensis* **2019**, *31*, 66−71.
(24) Talhout, R.; Opperhuizen, A.; van Amsterdam, J. G. C. Sugars as tobacco ingredient: Effects on mainstream smoke composition. *Food Chem. Toxicol.* **2006**, *44*, 1789−1798.
(25) Chen, T. T.; Zhang, H. J.; Zeng, R. E.; Wang, X. Y.; Huang, L. P.; Wang, L. D.; Wang, X. W.; Zhang, L. Shade Effects on Peanut Yield Associate with Physiological and Expressional Regulation on Photosynthesis and Sucrose Metabolism. *Int. J. Mol. Sci.* **2020**, *21*, 5284.
(26) Yamaguchi, N.; Suzuki, S.; Makino, A. Starch degradation by alpha-amylase in tobacco leaves during the curing process. *Soil Sci. Plant Nutr.* **2013**, *59*, 904−911.
(27) Dewey, R. E.; Xie, J. H. Molecular genetics of alkaloid biosynthesis in Nicotiana tabacum. *Phytochemistry* **2013**, *94*, 10−27.
(28) Dixon, R. A.; Achnine, L.; Kota, P.; Liu, C. J.; Reddy, M. S.; Wang, L. The phenylpropanoid pathway and plant defence-a genomics perspective. *Mol. Plant Pathol.* **2002**, *3*, 371−390.
(29) Hamberger, B.; Hahlbrock, K. The 4-coumarate:CoA ligase gene family in Arabidopsis thaliana comprises one rare, sinapate-activating and three commonly occurring isoenzymes. *Proc. Natl. Acad. Sci. U.S.A.* **2004**, *101*, 2209−2214.
(30) Wang, X.; Zhang, X. C.; Hou, H. X.; Ma, X.; Sun, S. L.; Wang, H. W.; Kong, L. R. Metabolomics and gene expression analysis reveal the accumulation patterns of phenylpropanoids and flavonoids in different colored-grain wheats (Triticum aestivum L.). *Food Res. Int.* **2020**, *138*, 109711.
(31) Guo, Y. F.; Hiatt, E.; Bonnet, C.; Kudithipudi, C.; Lewis, R. S.; Shi, H. Z.; Patra, B.; Zhao, X.; Dorlhac de Borne, F. D.; Gilles, T.; Yang, S. M.; Zhang, H. B.; Zhang, M. Y.; Lusso, M.; Berger, I. J.; Xu, D. M.; Wen, L. Y. Molecular regulation and genetic manipulation of alkaloid accumulation in tobacco plants. *Stud. Nat. Prod. Chem.* **2021**, *70*, 119−149.
(32) Saunders, J. A. Investigations of Vacuoles Isolated from Tobacco. *Plant Physiol.* **1979**, *64*, 74−78.
(33) Kaminski, K. P.; Bovet, L.; Laparra, H.; Lang, G.; De Palo, D.; Sierro, N.; Goepfert, S.; Ivanov, N. V. Alkaloid chemophenetics and transcriptomics of the Nicotiana genus. *Phytochemistry* **2020**, *177*, 112424.
(34) Shi, Q. X.; He, Y. R.; Chen, J.; Lu, L. H. Thermally Induced Actinidine Production in Biological Samples. *J. Agric. Food Chem.* **2020**, *68*, 12252−12258.
(35) Omar, H.; Fadaeinasab, M.; Taha, H.; Widyawaruyanti, A.; Nafiah, M. A.; Rachmatiah, T. Aporphine alkaloids with in vitro antiplasmodial activity from the leaves of Phoebe tavoyana. *J. Asian Nat. Prod. Res.* **2020**, *22*, 52−60.
(36) Yang, B.; Li, H. W.; Qiao, Y.; Zhou, Q.; Chen, S. P.; Yin, D.; He, H.; He, M. Tetramethylpyrazine Attenuates the Endotheliotoxicity and the Mitochondrial Dysfunction by Doxorubicin via 14-3-3γ/Bcl-2. *Oxid. Med. Cell. Longev.* **2019**, *2019*, 5820415.
(37) Zhao, L.; Li, W.; Wang, B.; Gao, Y.; Sui, X.; Liu, Y.; Chen, X.; Yao, X.; Jiao, F.; Song, Z. Development of a PVY Resistant Flue-Cured Tobacco Line via EMS Mutagenesis of eIF4E. *Agronomy* **2020**, *10*, 36.
(38) Wellburn, A.; Lichtenthaler, H. Formulae and program to determine total carotenoids and chlorophylls a and b of leaf extracts in different solvents. *Advances in Photosynthesis Research*; Springer: Dordrecht, 1984; pp 9−12.
(39) Neff, M. M.; Chory, J. Genetic Interactions between Phytochrome A, Phytochrome B, and Cryptochrome 1 during Arabidopsis Development1. *Plant Physiol.* **1998**, *118*, 27−35.
(40) Kong, D. X.; Li, Y. Q.; Bai, M.; He, H. J.; Liang, G. X.; Wu, H. Correlation between the dynamic accumulation of the main effective components and their associated regulatory enzyme activities at different growth stages in Lonicera japonica Thunb. *Ind. Crop. Prod.* **2017**, *96*, 16−22.
(41) Ganzera, M.; Zhao, J.; Khan, I. Hypericum perforatum-Chemical profiling and quantitative results of St. John's Wort products by an improved high-performance liquid chromatography method. *J. Pharm. Sci.* **2002**, *91*, 623−630.
(42) Carpentier, S. C.; Witters, E.; Laukens, K.; Deckers, P.; Swennen, R.; Panis, B. Preparation of protein extracts from recalcitrant plant tissues: An evaluation of different methods for two-dimensional gel electrophoresis analysis. *Proteomics* **2005**, *5*, 2497−2507.
(43) Zhu, W.; Han, H. T.; Liu, A. M.; Guan, Q. J.; Kang, J. N.; David, L.; Dufresne, D.; Chen, S. X.; Tian, J. K. Combined ultraviolet and darkness regulation of medicinal metabolites in Mahonia bealei revealed by proteomics and metabolomics. *J. Proteomics* **2021**, *233*, 104081.
(44) Zhong, Z. H.; Liu, S. Z.; Han, S. L.; Li, Y. H.; Tao, M. L.; Liu, A. M.; He, Q.; Chen, S. X.; Dufresne, D.; Zhu, W.; Tian, J. K. Integrative omic analysis reveals the improvement of alkaloid accumulation by ultraviolet-B radiation and its upstream regulation in Catharanthus roseus. *Ind. Crop. Prod.* **2021**, *166*, 113448.

https://doi.org/10.1021/acsomega.2c03877
ACS Omega 2022, 7, 33295−33306